

Isomerization of  $\alpha$ - and  $\beta$ -pinene epoxides over dendritic ZSM-5 zeolites

Carina Mosquera<sup>a</sup>, Luis A. Gallego-Villada<sup>b,\*</sup>, Marta Mediavilla<sup>a,c</sup>, Jennifer Cueto<sup>d</sup>,  
Maria del Mar Alonso-Doncel<sup>d</sup>, Edwin Alarcón<sup>a</sup>, David P. Serrano<sup>d,e,\*\*</sup>

<sup>a</sup> Environmental Catalysis Research Group, Chemical Engineering Faculty, Universidad de Antioquia, Medellín, Colombia

<sup>b</sup> Laboratory of Industrial Chemistry and Reaction Engineering, Johan Gadolin Process Chemistry Centre, Åbo Akademi University, Henriksgatan 2, 20500, Turku/ Åbo, Finland

<sup>c</sup> Engineering Faculty, Universidad Central de Venezuela, Caracas, Venezuela

<sup>d</sup> Thermochemical Processes Unit, IMDEA Energy Institute, Avda. Ramón de la Sagra, 3, 28935, Móstoles, Madrid, Spain

<sup>e</sup> Chemical and Environmental Engineering Group, Rey Juan Carlos University, c/Tulipán s/n, 28933, Móstoles, Madrid, Spain

## ARTICLE INFO

## Keywords:

Green metrics  
Kinetic modelling  
Campholenic aldehyde  
Carveol  
Myrtanal  
Dendritic zeolite

## ABSTRACT

The selective isomerization of  $\alpha$ - and  $\beta$ -pinene epoxides was investigated using dendritic ZSM-5 zeolite catalysts under mild reaction conditions using ethyl acetate as solvent at moderate temperatures (40–70 °C). The highly interconnected dendritic meso-macroporous structure and suitable Brønsted-to-Lewis acid sites balance facilitated efficient epoxide ring opening and rearrangement pathways without the need for additional metal functionalization as active phases. Likewise, the dendritic samples exhibited a superior catalytic activity than a reference hierarchical ZSM-5 material.  $\alpha$ -Pinene epoxide reaction yielded mainly campholenic aldehyde and carveol derivatives, while  $\beta$ -pinene epoxide rearranged to myrtanal, perillyl alcohol, and myrtenol. The metal-free nature of the catalyst offers advantages in terms of sustainability and product purity, making it a promising alternative for fine chemical synthesis from renewable terpene resources. Green metrics were calculated for the isomerization of both epoxides, such as atom economy, yield, stoichiometric factor, material recovery parameter, and reaction mass efficiency, demonstrating the green credentials of the process. The kinetic study of  $\alpha$ -pinene epoxide into campholenic aldehyde provided an activation energy of 75.6 kJ·mol<sup>-1</sup>. For  $\beta$ -pinene epoxide, the cis- and trans-myrtanal isomers dominate, exhibiting activation energies of 62.0 and 64.4 kJ·mol<sup>-1</sup>, respectively. The adsorption of cis- and trans-myrtanal onto the catalyst surface significantly influenced the product distribution of the transformation of  $\beta$ -pinene epoxide over the dendritic zeolite catalyst.

## 1. Introduction

In recent years, obtaining value-added chemicals from renewable raw materials has gained relevance in green chemistry. This has led to the development of sustainable alternatives seeking to enhance the use of natural products in industry. Terpenes, present as secondary metabolites in plants, represent the most extensive class of natural compounds and play a fundamental role as precursors in synthesizing various valuable chemicals. [1,2] Among them,  $\alpha$ - and  $\beta$ -pinene, which are terpenes obtained from turpentine oil, can be epoxidized at the carbon-carbon double bond, leading to  $\alpha,\beta$ -pinene epoxides. [3,4]

These epoxides are highly versatile organic compounds that act as key intermediates in various fine chemical processes. Due to the high reactivity of these epoxides, caused by the strain of the oxirane ring and

the polarization of the carbon-oxygen bonds, ring opening can be promoted, resulting in the reorganization into more thermodynamically stable compounds that have potential applications in the fragrance, flavour, and pharmaceutical industries. [5,6] The rearrangement or isomerization of  $\alpha$ -pinene epoxide typically yields products such as carveol, campholenic aldehyde, and fencholenic aldehyde, along with low selectivity to pinocarveol, and p-cymene. [7,8]. On the other hand, the isomerization of  $\beta$ -pinene epoxide has led to the formation of myrtanal, myrtenol, and perillyl alcohol as major products. However, perillyl aldehyde, isoperillyl alcohol, and anthemol have also been reported as possible products. [6,9]

The basicity and polarity of the solvent, as well as the acidity of the catalyst (Lewis or Brønsted), have a crucial role in the selectivity of the isomerization of  $\alpha$ - and  $\beta$ -pinene epoxides. In the case of  $\alpha$ -pinene oxide,

\* Corresponding author.

\*\* Correspondence to: D.P. Serrano, Thermochemical Processes Unit, IMDEA Energy Institute, Avda. Ramón de la Sagra, 3, 28935, Móstoles, Madrid, Spain.

E-mail addresses: [alfonso.gallego@udea.edu.co](mailto:alfonso.gallego@udea.edu.co) (L.A. Gallego-Villada), [david.serrano@imdea.org](mailto:david.serrano@imdea.org) (D.P. Serrano).

<https://doi.org/10.1016/j.cej.2026.174355>

Received 2 December 2025; Received in revised form 30 January 2026; Accepted 17 February 2026

Available online 18 February 2026

1385-8947/© 2026 The Author(s). Published by Elsevier B.V. This is an open access article under the CC BY-NC-ND license (<http://creativecommons.org/licenses/by-nc-nd/4.0/>).

it has been found that the use of non-polar solvents and catalysts with Lewis sites promotes the formation of campholenic aldehyde with high selectivity, while systems with polar solvents and Brønsted acid catalysts favour the formation of carveol. [8,10] For example, the Ti-beta-PS-HT-Li system, a dealuminated beta zeolite modified with titanium via a post-synthetic route, hydrothermally treated and partially exchanged with lithium ions, achieved a conversion of 99.1% with a selectivity of 87.3% towards campholenic aldehyde in acetone at 150 °C. Likewise, the Ce/SiO<sub>2</sub> catalyst in a polar medium (dimethylacetamide) showed high conversion (99.3%) and favoured the formation of trans-carveol (72%). In another study, the use of Ti/MCM-22 catalyst in toluene at 70 °C led to a high selectivity towards campholenic aldehyde (96% at the total conversion). [11] Conversely, systems employing polar solvents and Brønsted acid catalysts often promote the formation of carveol and related alcohols through a proton-assisted epoxide opening mechanism. A notable example is the 32 wt% Ce-Si-MCM-41 catalyst using *N*-methylpyrrolidone as a solvent, which leads to 46% of selectivity at total conversion of  $\alpha$ -pinene oxide. [12] In the isomerization of  $\beta$ -pinene oxide, it has been observed that the use of polar solvents and catalysts with Lewis acid sites significantly improves selectivity towards the formation of myrtanal, compared to non-polar solvents and catalysts with Brønsted acid sites, which tend to favour the formation of perillyl alcohol. [13] This behaviour is confirmed in studies where catalysts, such as Sn-MCM-41 (with nitromethane as solvent), Fe/SBA-15 (acetonitrile as solvent) and Zr-Beta Zeolite (acetonitrile as solvent), achieve conversions greater than 98%, showing selectivity towards myrtanal of 66%, 85%, and 94%, respectively. In contrast, catalysts like Ti/SBA-15, also using a non-polar solvent (hexane), exhibit higher selectivity towards perillyl alcohol (45%) with conversions up to 99%. [14,15] These results demonstrate how the proper choice of solvent and the type of acidity of the catalyst can direct the reaction towards specific products. [16,17]

In recent works, the synthesis of dendritic ZSM-5 zeolite (d-ZSM-5) has been reported, exhibiting singular properties. These materials present three-dimensional branched nano-structures with radial intraparticle orientation and a highly interconnected multilevel porosity. As a consequence, dendritic ZSM-5 zeolite shows exceptional accessibility to the active sites of the catalyst, [18,19] located both within the micropores and on the external surface of crystalline nano-units. These features are particularly advantageous in biomass valorisation processes and in the synthesis of high-value-added products, where the substrates and/or intermediates often involve bulky molecules. Moreover, from a chemical standpoint, dendritic ZSM-5 exhibits a well-balanced distribution of Brønsted and Lewis acid sites, the latter being generated by aluminium species in octahedral coordination, without requiring the addition of metal species as active centres. Depending on the reaction, this may represent a significant advantage over other catalytic materials, such as supported metal oxides or functionalized solids, which typically require impregnation with metal species (e.g., Fe, Ti, Sn, Zr) to generate Lewis acid sites. Altogether, the synergy between structural accessibility and acid site distribution makes d-ZSM-5 an outstanding catalytic platform, markedly more versatile, efficient, and sustainable than most solid catalysts reported in the literature for the isomerization of monoterpene epoxides. [18–21]

In a previous investigation, the isomerization of  $\alpha$ -pinene and  $\beta$ -pinene epoxides was evaluated using a dendritic zeolite ZSM-5 as a catalyst [18]. The zeolite showed significantly superior performance compared to conventional and hierarchical zeolites due to its high accessibility and large concentration of acid sites on the external surface. The reactions were carried out under mild conditions, using ethyl acetate as a solvent, at 60 °C and 50 °C for the isomerization of  $\alpha$ - and  $\beta$ -pinene epoxides, respectively, for 60 min. Under these conditions, the catalyst showed a complete conversion of both epoxides. These preliminary results validate the effectiveness of dendritic zeolites in the transformation of terpene epoxides. However, that study was focused only on catalytic screening under a single set of reaction conditions. No

kinetic analysis, systematic variation of operating parameters, nor assessment of green metrics was conducted. These important issues are now addressed in the present work.

The current study further evaluates the catalytic behaviour of dendritic ZSM-5 zeolite in the isomerization of  $\alpha$ - and  $\beta$ -pinene epoxides with the aim of getting essential information for this process to be applied on a large scale. Thereby, the current work focused on the effect of the textural properties and acidity of the dendritic zeolites, the modelling of the transformation pathways kinetics, the reuse/regeneration of the catalyst and the sustainability assessment of the process through a number of green metrics parameters, such as atom economy (AE), reaction yield ( $\epsilon$ ), stoichiometric factor (SF), material recovery parameter (MRP), reaction mass efficiency (RME), environmental factor (*E*-factor) and process mass intensity (PMI). The results here reported show that this type of catalytic system exhibits a remarkable performance towards value-added products such as campholenic aldehyde and myrtanal, achieving productivities significantly higher than those of previous catalytic systems reported in the literature. [22–24] The kinetic study provided valuable insights into the transformation routes of pinene epoxides, offering useful tools for process optimization, preliminary reactor design, and potential future scale-up. In addition, the green metrics parameters demonstrate the potential of the catalytic system for sustainable application in future chemical processes.

## 2. Materials and methods

### 2.1. Materials

Tetraethyl orthosilicate (TEOS, Sigma-Aldrich, 98 wt%) was used as the silicon source, aluminium isopropoxide (AIP, Sigma-Aldrich, 98 wt %) as the aluminium source, tetrapropylammonium hydroxide (TPAOH, Sigma-Aldrich, 40 wt% in water) as the structure-directing agent, *N*-[3-(trimethoxysilyl)propyl]aniline (Ph-A, Sigma-Aldrich, 98%), and dime-thyldecyl[3-(trimethoxysilyl)propyl]ammonium chloride (TPOAC, Sigma-Aldrich, 42 wt% in methanol) as an amphiphilic organosilane for the generation of the dendritic nanoarchitecture in ZSM-5 zeolite.  $\alpha$ -Pinene epoxide (97 wt%, Sigma-Aldrich),  $\beta$ -pinene epoxide (97 wt%, synthesized according to a previously described procedure [25]), and ethyl acetate (anhydrous, 99.8 wt%, Sigma-Aldrich) were used as the reagents for the catalytic tests.

### 2.2. Synthesis of ZSM-5 zeolites

The dendritic zeolite ZSM-5 (d-ZSM-5) and hierarchical zeolite (h-ZSM-5) samples were synthesized via a hydrothermal crystallization method, as earlier described. [18,19] For d-ZSM-5 materials, a precursor gel with a molar composition of 1 Al<sub>2</sub>O<sub>3</sub>:60 SiO<sub>2</sub>:11 TPAOH:1500H<sub>2</sub>O was prepared by dissolving AIP in a TPAOH/water solution, followed by the gradual addition of TEOS. After complete hydrolysis and removal of alcohol by vacuum evaporation, the clear solution underwent a pre-crystallization step at 90 °C for 20 h. Once cooled, TPOAC (5 mol% relative to Si) was added, and the mixture was stirred at 0 °C for 6 h before being transferred to a Teflon-lined reactor. Hydrothermal crystallization was conducted at 150 °C for 4 or 7 days (d-ZSM-5/4d or d-ZSM-5/7d, respectively). The solid product was recovered by washing, centrifugation, and drying, and finally calcined through a two-step (N<sub>2</sub>/air) process in a tubular furnace. In the first step, d-ZSM-5 zeolite was heated with a ramp of 1.8 °C min<sup>-1</sup> to 400 °C under nitrogen flow (100 mL·min<sup>-1</sup>), maintaining this temperature constant for 4 h. Subsequently, the sample was heated up to 550 °C with a 1.8 °C min<sup>-1</sup> ramp under air flow (100 mL min<sup>-1</sup>), keeping this temperature for 5 h.

The hierarchical zeolite h-ZSM-5 was synthesized using a modified procedure of that for d-ZSM-5 samples. Thus, after the pre-crystallization step, 5 mol% of Ph-A was added to the gel, which was maintained at 90 °C and stirred under reflux for 6 h. The mixture was then subjected to hydrothermal crystallization at 170 °C for 7 days.

Upon completion, the solid product was separated from the clear supernatant, recovered, and activated following the same post-treatment steps as for d-ZSM-5.

### 2.3. Catalyst characterization

The catalysts were extensively characterized by established techniques such as X-ray diffraction (XRD), textural analysis, Transmission Electron Microscopy (TEM), High Resolution Scanning Electron Microscopy (HR-SEM), and infrared spectroscopy using pyridine and 2,6-di-tert-butylpyridine (DTBP) as probe molecules, as detailed in Gallego-Villada et al. (2024). [18] These techniques allowed for the assessment of structural, textural, and acidic properties of the materials.

### 2.4. Tests of $\alpha$ - and $\beta$ -pinene epoxides isomerization

The isomerization of  $\alpha$ - and  $\beta$ -pinene epoxides was carried out in batch reactors (small vials), which were sealed with inert silicon septa and immersed in a Radley Tech StarFish Multi-Experiment Workstation hotplate, under magnetic stirring. In a typical experiment, a specific amount of catalyst (7–16 mg) was mixed with 1 mL and 0.5 mL of a solution of  $\alpha$ -pinene or  $\beta$ -pinene epoxide, respectively, in ethyl acetate, with a concentration of 0.25 M. The mixture was heated to temperatures between 40 °C and 70 °C for reaction times ranging from 5 to 120 min under stirring at 750 rpm. Upon completion, the catalyst was separated by centrifugation (3000 rpm), and the liquid phase was analysed by gas chromatography coupled with mass spectrometry (GC–MS) using an Agilent Technologies GC/MS 7890A/5975C system. Separation was performed on a DB-1 column (30 m length  $\times$  320  $\mu$ m internal diameter  $\times$  0.25  $\mu$ m film thickness), with helium as the carrier gas at a flow rate of 2.3 mL min<sup>−1</sup> and a pressure of 0.110 MPa, using a split ratio of 25:1. Injections of 1  $\mu$ L were carried out using an autosampler, and detection was performed with a flame ionization detector (FID) at 250 °C. The oven temperature program consisted of an initial ramp from 70 °C to 90 °C at 10 °C min<sup>−1</sup> (held for 0.5 min), followed by an increase up to 110 °C (10 °C min<sup>−1</sup>, 0.5 min), then to 130 °C (10 °C min<sup>−1</sup>, 0.5 min), and finally to 160 °C (15 °C min<sup>−1</sup>, held for 1 min). Compound identification was performed by comparison with the NIST 5 database.

The conversion of  $\alpha$ - and  $\beta$ -pinene oxide epoxides ( $X_i$ ) and the selectivity towards product  $j$  ( $S_j$ ) were determined using Eqs. (1) and (2), respectively:

$$X_i = \frac{C_{i,0} - C_{i,t}}{C_{i,0}} \times 100 \quad (1)$$

$$S_j = \frac{C_{j,t}}{\sum C_{j,t}} \times 100 \quad (2)$$

where  $C_{i,0}$ ,  $C_{i,t}$ , and  $C_{j,t}$  refer to the initial concentration of epoxide, concentration of epoxide after time  $t$ , and the concentration of the product  $j$  after time  $t$  in the reaction mixture, respectively.

TOF for  $\alpha$ - and  $\beta$ -pinene epoxide conversion was calculated using Eq. (3).

$$\text{TOF} = \frac{n_{i,0} - n_{i,t}}{\Delta t \times \text{TA} \times W} \quad (3)$$

where  $n_{i,0}$  and  $n_{i,t}$  refer to the mole of epoxide in initial time (0 min) and after 5 min, respectively;  $\Delta t$  denotes the elapsed reaction time;  $W$  is the mass of catalyst used; and  $\text{TA}$  indicates the total acidity, calculated as the sum of the Brønsted and Lewis acid sites concentration of the catalyst.

### 2.5. Leaching and reusability tests

The leaching and reuse/regeneration tests were evaluated with 10 mg of catalyst and 0.25 M of  $\alpha$ - and  $\beta$ -pinene oxides in ethyl acetate at

70 °C. For the leaching test, after 5 min, the catalyst was removed from the mixture using an Advantec syringe filter with a pore size of 0.45  $\mu$ m. An aliquot was taken for analysis using GC–MS. The filtration was used to proceed with the reaction, and aliquots were taken for GC–MS analysis at 15, 30, 45, and 60 min of reaction. For the reuse cycle, the recovered catalyst was assessed using a fresh reaction mixture. For the regeneration test, the catalyst was separated by centrifugation at 3000 rpm for 5 min, washed with ethanol, dried at 80 °C for 2 h, and finally calcined at 400 °C (1.8 °C min<sup>−1</sup>, 4 h) and 550 °C (1.8 °C min<sup>−1</sup>, 5 h).

### 2.6. Kinetic modelling

#### 2.6.1. Reaction pathway

Table S1 summarizes the experimental runs used for the kinetic modelling of  $\alpha$ -pinene epoxide (APO) and  $\beta$ -pinene epoxide (BPO) isomerization. The reaction pathways for the isomerization of APO and BPO over the dendritic ZSM-5 zeolite were proposed according to the different products identified after the reaction tests (Fig. 1) using different reaction conditions (Supporting Information, Figs. S1 to S4). The reaction was confirmed to proceed under kinetic control at the tested conditions (Table S1) by verifying the absence of internal mass-transfer limitations using the Weisz-Prater criterion [26,27], as detailed in section 3 of the Supporting Information (Tables S2 and S3). In addition, the catalytic tests were performed with a high liquid volume-to-catalyst mass ratio and vigorous agitation (750 rpm) to suppress external mass/heat-transfer limitations [19].

For the  $\alpha$ -pinene epoxide, the reaction network primarily yields three main products: campholenic aldehyde (CA), carveol (COL), and fencholenic aldehyde (FA), with selectivities around 95%. Byproducts, accounting for approximately 5%, consist of epoxide isomers (C<sub>10</sub>H<sub>16</sub>O), collectively labelled as ‘other products’. These include trans-pinocarveol (PC), isopinocampheol (IPC), and dieneol (DOL). Additionally, p-cymene (Cy, C<sub>10</sub>H<sub>14</sub>) is formed through the dehydration of oxygenated compounds. Regarding the  $\beta$ -pinene epoxide, the reaction yields four products with a selectivity above 88%, corresponding to trans-myrtanal (TMAL), cis-myrtanal (CMAL), perillyl alcohol (PA), and myrtenol (MOL). The by-products, which account for a maximum of 12%, are epoxide isomers (C<sub>10</sub>H<sub>16</sub>O), also classified as “other products”.

#### 2.6.2. Kinetic equations

Two different kinetic models were evaluated for the isomerization of  $\alpha$ -pinene epoxide and  $\beta$ -pinene epoxide, considering both unimolecular and bimolecular surface reactions. The unimolecular mechanism was proposed based on our recent findings reported for the isomerization of limonene-1,2-epoxide over a dendritic zeolite [19]. In contrast, the bimolecular model, in which two adsorbed epoxide molecules interact to produce various surface reactions, was proposed based on the curvature observed in the experimental data, particularly at low temperatures. This bimolecular mechanism can be interpreted as a cooperative surface effect, in which an epoxide molecule first adsorbs onto an active site of the catalyst, with the subsequent ring rearrangement assisted by a neighboring adsorbed epoxide molecule, leading to an apparent bimolecular kinetic behaviour, even though the isomerization itself remains an intramolecular process mediated by the catalyst surface. A detailed derivation for both models is provided in Section 4 of the Supporting Information.

The general reaction rate expressions for the best-fitting kinetic model of  $\alpha$ -pinene epoxide isomerization are shown in Eqs. (4)–(5). This model includes bimolecular mechanisms for three of the surface reactions (formation of campholenic aldehyde, carveol, and fencholenic aldehyde) and a unimolecular mechanism for the formation of the other products (see Section 4.1.2 in the Supporting Information for further details). In contrast, the general rate expression for the isomerization of  $\beta$ -pinene epoxide is given in Eq. (6), in which all five reactions are described by a bimolecular mechanism (see Section 4.2.1 in the Supporting Information for further details). For both epoxides, the surface

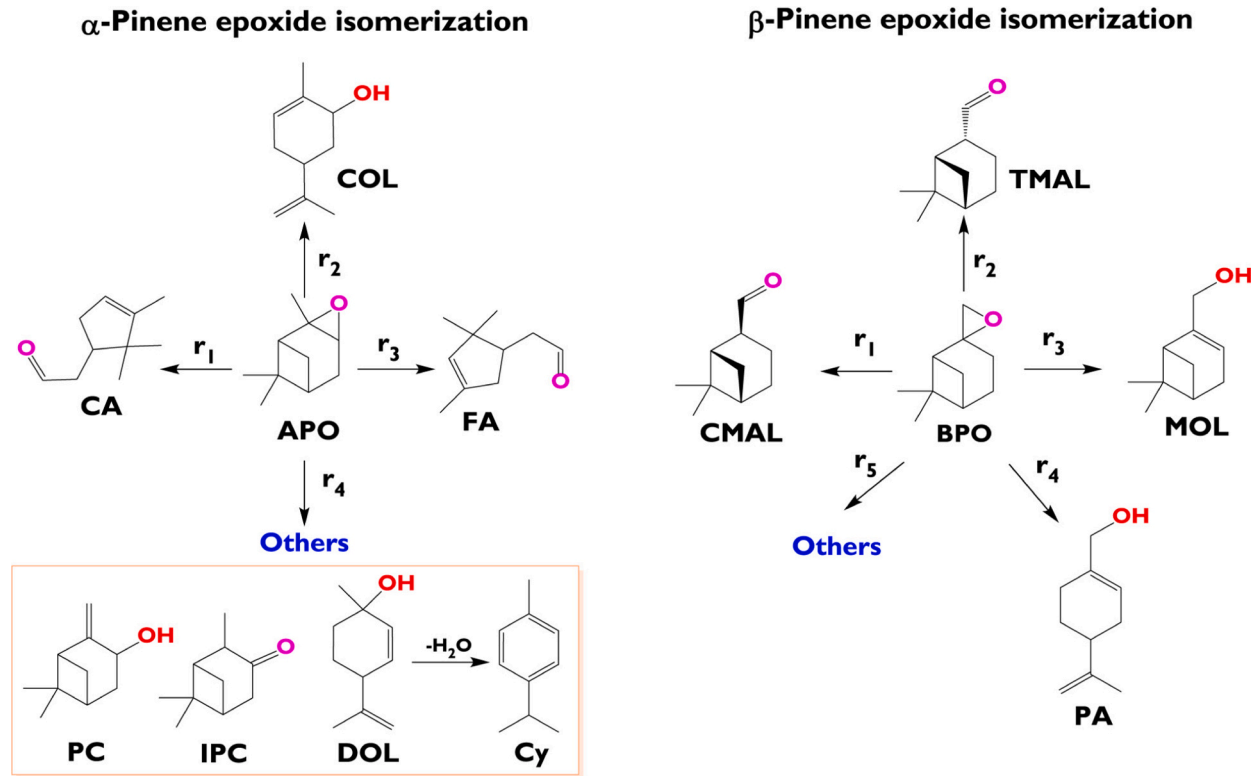


Fig. 1. Reaction networks for the isomerization of  $\alpha$ -pinene and  $\beta$ -pinene epoxides:  $\alpha$ -pinene epoxide (APO), campholenic aldehyde (CA), carveol (COL), fencholenic aldehyde (FA), trans-pinocarveol (PC), isopinocampheol (IPC), dienol (DOL), p-cymene (Cy),  $\beta$ -pinene epoxide (BPO), trans-myrtanal (TMAL), cis-myrtanal (CMAL), perillyl alcohol (PA), and myrtenol (MOL).

reactions are assumed to be irreversible, where  $k$  and  $K$  denote the reaction rate and adsorption equilibrium constants, respectively. The reaction constants are determined using the modified Arrhenius equation, Eq. (7), as described in the literature. [28,29] Here,  $k_{ref}$  represents the reaction rate constant at a reference temperature ( $T_{ref} = 60^\circ\text{C}$ ),  $E_a$  denotes the activation energy, and  $R$  is the gas constant. Additionally, the adsorption constants were assumed to remain constant within a small temperature range ( $40\text{--}70^\circ\text{C}$ ) [26,27], thereby avoiding the inclusion of an excessive number of parameters in the mathematical fitting.

$$r_i = \frac{k_i C_{APO}^2}{(1 + K_{APO} C_{APO} + K_{CA} C_{CA} + K_{COL} C_{COL} + K_{FA} C_{FA})^2} \quad (i = 1, 2, 3) \quad (4)$$

$$r_i = \frac{k_i C_{APO}}{1 + K_{APO} C_{APO} + K_{CA} C_{CA} + K_{COL} C_{COL} + K_{FA} C_{FA}} \quad (i = 4) \quad (5)$$

$$r_i = \frac{k_i C_{BPO}^2}{(1 + K_{BPO} C_{BPO} + K_{CMAL} C_{CMAL} + K_{TMAL} C_{TMAL} + K_{MOL} C_{MOL} + K_{PA} C_{PA})^2} \quad (i = 1, 2, 3, 4, 5) \quad (6)$$

$$k = k_{ref} e^{-\frac{E_a}{R} \left( \frac{1}{T} - \frac{1}{T_{ref}} \right)} \quad (7)$$

The mole balance for the species in the liquid phase in the batch reactor is represented by Eq. (8), where  $C_j$  is the concentration of species  $j$ ,  $V$  is the reaction volume,  $m_{cat}$  is the catalyst mass, and  $R_j$  is the production rate for species  $j$ , as shown in Table 1.

$$\frac{dC_j}{dt} = \frac{m_{cat}}{V} R_j \quad (8)$$

Table 1

Production rate for each species  $j$ .

$\alpha$ -Pinene epoxide (APO)		$\beta$ -Pinene epoxide (BPO)	
Specie	Production rate ( $R_j$ )	Specie	Production rate ( $R_j$ )
$\alpha$ -Pinene epoxide (APO)	$-r_1 - r_2 - r_3 - r_4$	$\beta$ -Pinene epoxide (BPO)	$-r_1 - r_2 - r_3 - r_4 - r_5$
Campholenic aldehyde (CA)	$r_1$	cis-Myrtanal (CMAL)	$r_1$
Carveol (COL)	$r_2$	trans-Myrtanal (TMAL)	$r_2$
Fencholenic aldehyde (FA)	$r_3$	Myrtenol (MOL)	$r_3$
Other products	$r_4$	Perillyl alcohol (PA)	$r_4$
		Other products	$r_5$

### 2.6.3. Parameters estimation

The estimation of parameters was carried out by nonlinear regression using the ModEst modelling and parameter estimation software. [30,31] This method minimizes the objective function by employing the Levenberg-Marquardt algorithm. The objective function (Eq. (9)) is defined as the squared difference between the experimental concentrations ( $C_{j,i,Exp}$ ) and the calculated concentrations ( $C_{j,i,Calc}$ ) of the species. The coefficient of determination ( $R^2$ ), a metric used for evaluating goodness of fit, was calculated based on the definition provided elsewhere. [19]

$$O.F. = \sum_j \sum_{i=1}^{N_{obs}} (C_{j,i,Exp} - C_{j,i,Calc})^2 \quad (9)$$



### 3. Results and discussion

#### 3.1. Catalyst characterization

The textural and acid properties of the catalysts are summarized in Table S4. A detailed description of the characterization techniques and procedures can be found in previous studies. [18–21] The h-ZSM-5 catalyst exhibits a lower proportion of mesopores (73.8%) and a smaller external mesoporous surface area ( $279 \text{ m}^2 \text{ g}^{-1}$ ) compared to the dendritic catalysts, which reach external mesoporous surface areas of  $360 \text{ m}^2 \text{ g}^{-1}$  and meso-macro porosity percentages above 79%. Regarding pore volume, h-ZSM-5 shows a total pore volume of  $0.66 \text{ cm}^3 \text{ g}^{-1}$  and a micropore volume of  $0.17 \text{ cm}^3 \text{ g}^{-1}$ . In contrast, d-ZSM-5/4d and d-ZSM-5/7d exhibit total pore volumes of  $0.68 \text{ cm}^3 \text{ g}^{-1}$ , with micropore volumes of 0.13 and  $0.14 \text{ cm}^3 \text{ g}^{-1}$ , respectively. These values indicate a higher contribution from mesopores in the dendritic catalysts, which may facilitate the diffusion of reactants and products through the material, minimizing steric and transport limitations typically associated with conventional microporous zeolites. In terms of acidity, all catalysts exhibit a higher concentration of Brønsted acid sites compared to Lewis sites; however, this difference is more pronounced in h-ZSM-5 (BA/LA = 3.1), while the dendritic catalysts show a more moderate ratio (BA/LA = 1.4 and 1.5). The dendritic materials, and in particular the d-ZSM-5/4d catalyst, show high accessibility to external acid sites, indicating greater exposure of Brønsted sites to the reactive environment.

The larger mesoporosity and accessibility observed in the dendritic catalysts are closely related to their distinctive morphological architecture. As shown in the TEM and HR-SEM micrographs in Fig. 2, the d-ZSM-5 zeolite samples exhibit an oval-shaped morphology of approximately  $400 \times 250 \text{ nm}$ , composed of 5–10 nm nano-units arranged in radially oriented and branched aggregates. This nano-architecture gives rise to a highly interconnected hierarchical pore network, including micropores, mesopores, and internal vesicles, which are expected to facilitate an efficient molecular transport, enhancing the catalytic potential of the material. Some core-shell organization, with a denser inner part, can be observed in the TEM images, mostly for the dendritic sample obtained after 7 days of crystallization. Conversely, the h-ZSM-5 sample features are loosely organized, spherical aggregates between 250 and 300 nm, made up of similarly sized nanoparticles. This disordered assembly produces mesopores with a broader range and less consistent pore dimensions. [18,19]

#### 3.2. Epoxide conversion and production distribution

Fig. 3 shows the evolution of the conversion of  $\alpha$ - and  $\beta$ -pinene epoxides over time, using a hierarchical (h-ZSM-5) and two dendritic (d-ZSM-5/4d and d-ZSM-5/7d) zeolite samples. With the three catalysts, the substrate conversions are higher for the  $\alpha$ -pinene epoxide, showing a lower reactivity of the  $\beta$ -pinene epoxide. On the other hand, the results indicate that the reaction of the epoxides is significantly faster with the d-ZSM-5/4d zeolite, followed by d-ZSM-5/7d, while h-ZSM-5 exhibits the lowest catalytic activity. It is remarkable that over the d-ZSM-5/4d catalyst, the reaction is so fast that a total conversion of both epoxides is achieved just in 10 min of reaction time. The behaviour of the three catalysts can be related to key structural differences among the materials. In particular, dendritic zeolites exhibit a higher mesopore/external surface area than the hierarchical zeolite (360, 330, and  $279 \text{ m}^2 \text{ g}^{-1}$  for d-ZSM-5/7d, d-ZSM-5/4d, and h-ZSM-5, respectively), which improves reactant accessibility to active sites and facilitates product transport. Additionally, the external Brønsted acid site concentration is considerably higher in the dendritic zeolites (97, 61, and  $41 \text{ } \mu\text{mol g}^{-1}$  for d-ZSM-5/7d, d-ZSM-5/4d, and h-ZSM-5, respectively), which increases the availability of accessible catalytic centres and thereby enhances the efficiency of the conversion process.

Fig. 4 shows the evolution of the selectivity towards campholenic aldehyde and myrtanal as the reaction progresses, using d-ZSM-5/7d, d-

ZSM-5/4d, and h-ZSM-5 zeolites as catalysts. It can be observed that d-ZSM-5/4d exhibits a somewhat lower selectivity at isoconversion conditions towards both compounds compared to the other two materials. According to the literature, [10,32] Lewis acid sites are more effective in promoting the transformation of epoxides into oxygenated compounds such as campholenic aldehyde and myrtanal. In this context, the higher concentration of external Brønsted sites in d-ZSM-5/4d could be related to its lower selectivity towards the desired oxygenated products, due to competition with other reaction pathways.

#### 3.3. Relationship between catalytic performance and zeolite properties

Fig. 5 shows the correlation between the turnover frequency (TOF) values for the isomerization of  $\alpha$ - and  $\beta$ -pinene epoxides and the concentration of Brønsted acid sites located on the external surface of the catalysts. Among the evaluated materials, the d-ZSM-5/4d catalyst exhibited the highest TOF values, attributed to a high density of externally accessible Brønsted acid sites, a relatively low BA/LA ratio, and a larger proportion of external mesopore area. These results indicate that catalytic performance is governed not only by the number of acid sites, but also by their accessibility, which is facilitated by the singular nano-architecture of dendritic materials that minimizes steric and diffusional limitations. Therefore, it can be concluded that proper engineering of the porous structure, together with an optimized acid balance, is key to improving catalytic performance in this type of reaction.

Table S5 compares the productivity towards campholenic aldehyde and myrtanal from the isomerization of  $\alpha$ - and  $\beta$ -pinene epoxides, respectively, using different catalysts based on literature data. In both systems, the productivity of the dendritic zeolites evaluated in this work is higher than that previously reported with other catalytic systems. In the case of  $\alpha$ -pinene epoxide, the zeolite d-ZSM-5/4d exhibited the highest productivity towards campholenic aldehyde ( $2.5 \text{ mmol g}^{-1} \text{ min}^{-1}$ ), followed by d-ZSM-5/7d and h-ZSM-5 (c.a.  $1.6 \text{ mmol g}^{-1} \text{ min}^{-1}$ ), demonstrating results significantly better than those obtained with other catalytic systems. A similar trend was observed in the isomerization of  $\beta$ -pinene epoxide, where d-ZSM-5/4d also showed the highest productivity ( $1.0 \text{ mmol g}^{-1} \text{ min}^{-1}$ ), followed by d-ZSM-5/7d ( $0.61 \text{ mmol g}^{-1} \text{ min}^{-1}$ ) and h-ZSM-5 ( $0.42 \text{ mmol g}^{-1} \text{ min}^{-1}$ ), compared to values below  $0.1 \text{ mmol g}^{-1} \text{ min}^{-1}$  reported for other catalysts. These differences become even more significant considering that the dendritic zeolites achieve such high productivity under mild operating conditions and without the use of metals as active phases, which represent significant advantages.

Although d-ZSM-5/4d proved to be the most active catalyst, the selectivity analysis revealed that d-ZSM-5/7d exhibited a better selectivity towards the desired products, achieving 73% for campholenic aldehyde from  $\alpha$ -pinene epoxide and 53% for myrtanal from  $\beta$ -pinene epoxide. In comparison, d-ZSM-5/4d reached selectivities of 57% and 47%, respectively. Accordingly, the d-ZSM-5/7d sample was selected to evaluate the influence of key reaction parameters, including temperature and catalyst loading, as is detailed in the Supporting Information (Section 2, Figs. S1–S4). Additionally, reversibility tests (Supporting Information, Section 7, Fig. S8) using carveol and perillyl alcohol as reagents were conducted. No changes were observed in the GC analyses under the tested conditions along the reaction time, showing that the reverse reactions do not occur.

#### 3.4. Reaction kinetics

##### 3.4.1. Kinetics of $\alpha$ -pinene epoxide transformation

The kinetic studies available in the literature for this reaction are still limited and generally fail to accurately reflect the true complexity of the system. For example, Salminen et al. (2014), [33] developed a first-order pseudo-homogeneous kinetic model for supported ionic liquid catalysts (SILCA), which considers five parallel reaction pathways leading to the formation of campholenic aldehyde, fencholenic

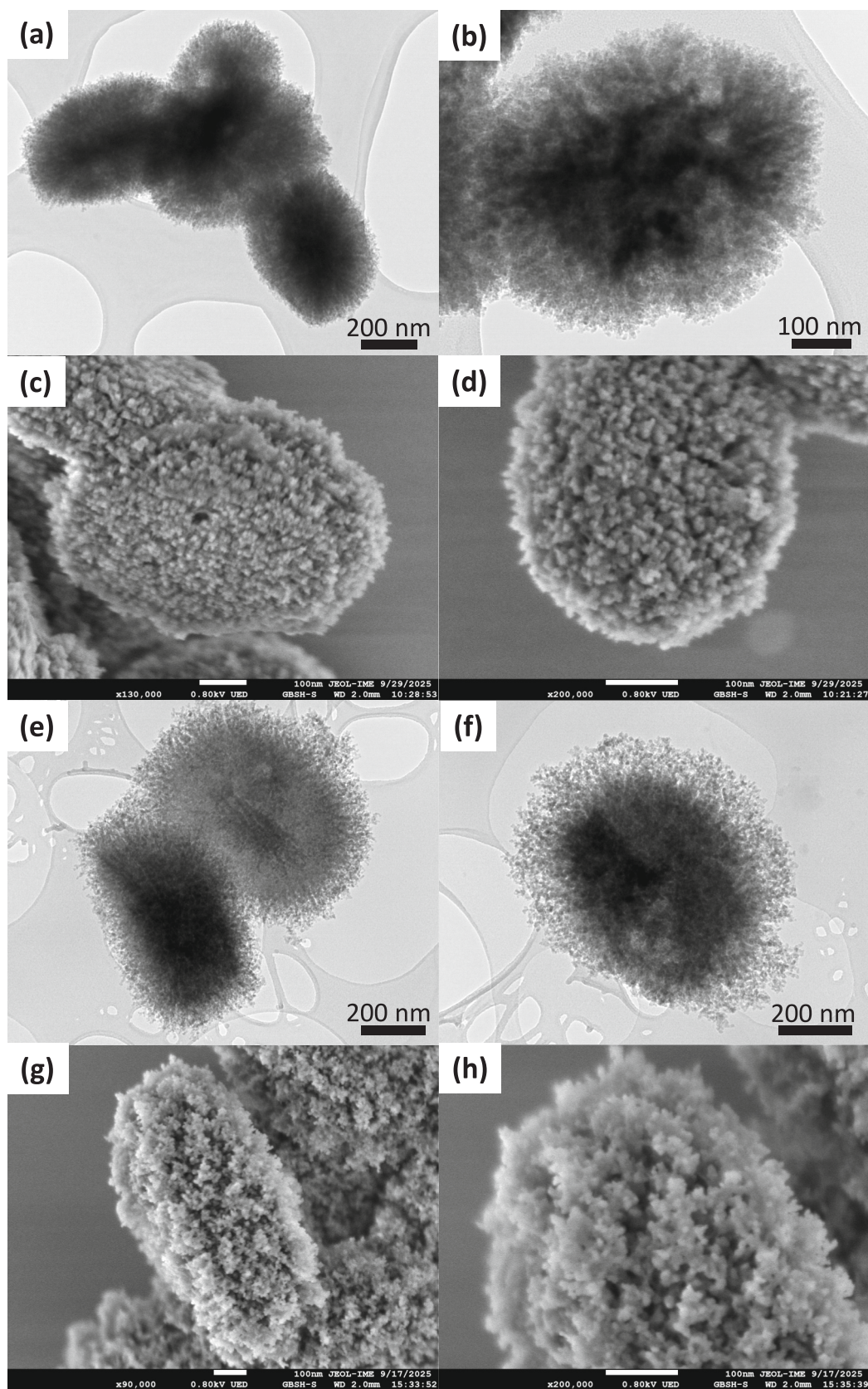
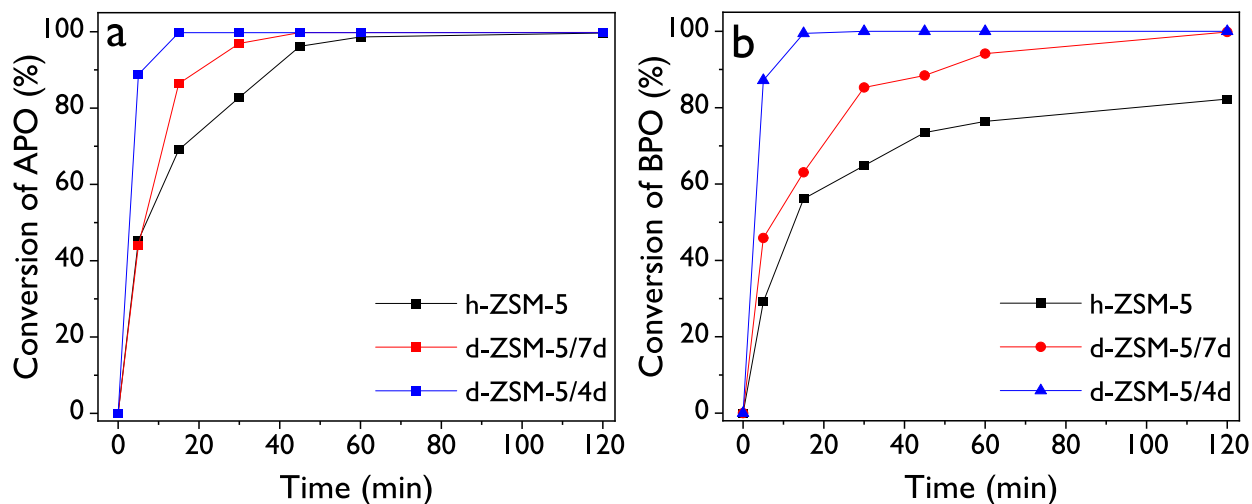
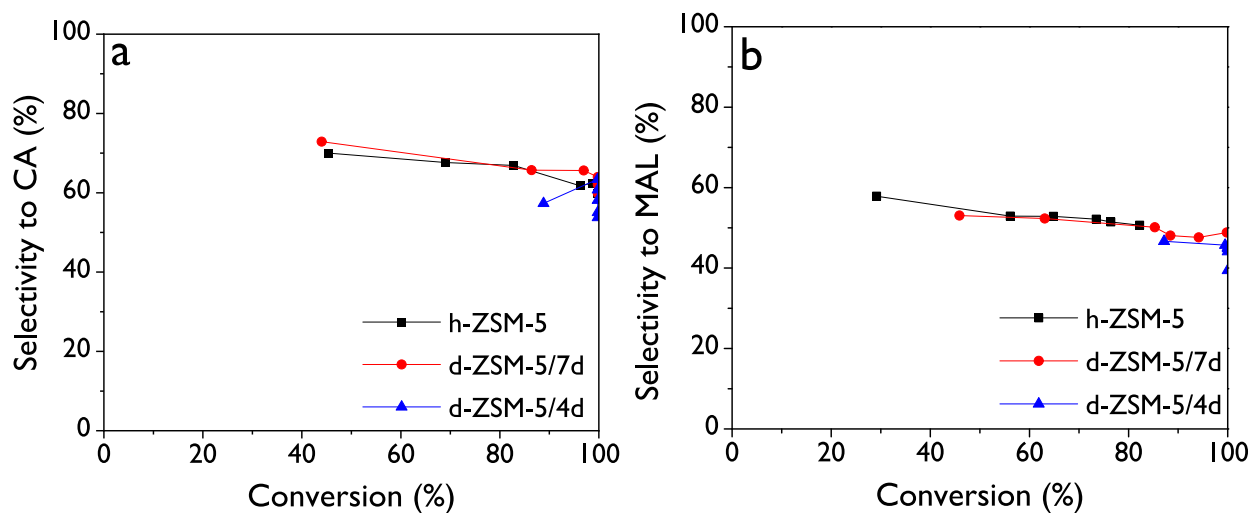


Fig. 2. TEM and HR-SEM micrographs of d-ZSM-5/4d (a-d), and d-ZSM-5/7d (e-h) samples.



**Fig. 3.** Conversion profiles for (a)  $\alpha$ -pinene epoxide and (b)  $\beta$ -pinene epoxide. Reaction conditions:  $C_{\text{epoxide}} = 0.25 \text{ mol L}^{-1}$ , ethyl acetate as the solvent, 10 mg of catalyst, 70 °C, 750 rpm.



**Fig. 4.** (a) Selectivity to campholenic aldehyde vs.  $\alpha$ -pinene epoxide conversion and (b) selectivity to myrtanal (cis + trans) vs.  $\beta$ -pinene epoxide conversion. Reaction conditions:  $C_{\text{epoxide}} = 0.25 \text{ mol L}^{-1}$ , ethyl acetate as the solvent, 10 mg of catalyst, 70 °C, 750 rpm.

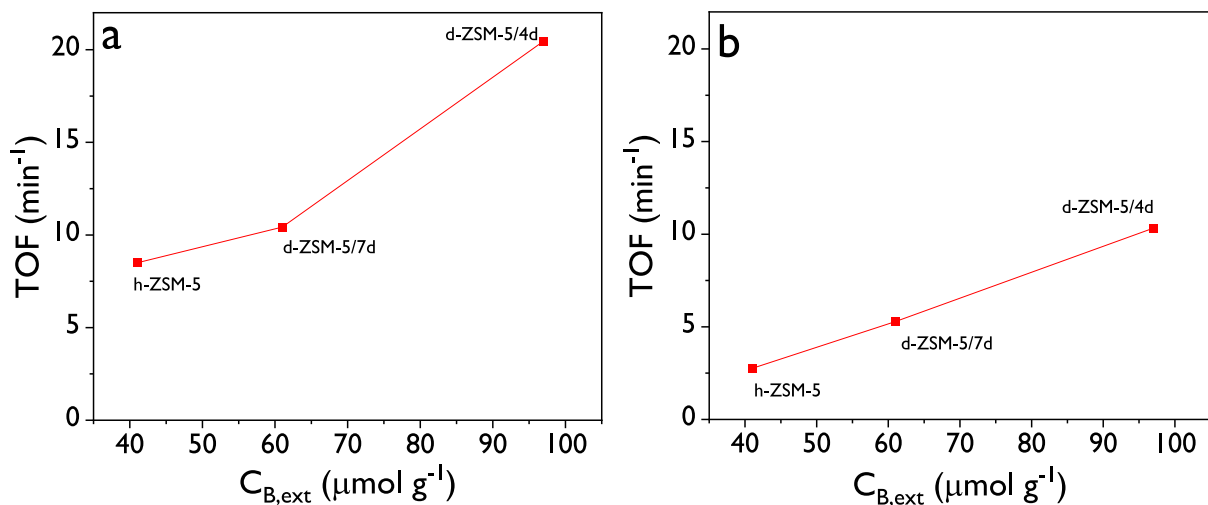


**Fig. 5.** Turnover frequency (TOF) as a function of external Brønsted acidity in the transformation of (a)  $\alpha$ -pinene epoxide and (b)  $\beta$ -pinene epoxide. Reaction conditions:  $C_{\text{epoxide}} = 0.25 \text{ mol L}^{-1}$ , ethyl acetate as the solvent, 10 mg of catalyst, 70 °C, 5 min, 750 rpm.



aldehyde, trans-carveol, isopinocampheol, and pinocarveol. In another study, Sánchez-Velandia et al. (2019), [34] examined the same reaction using three different kinetic approaches: a pseudo-homogeneous model, a Langmuir–Hinshelwood–Hougen–Watson (LHHW) type model, and LHHW model considering a dual-site adsorption applied to iron-modified mesoporous catalysts. Although the latter two approaches incorporated substrate adsorption effects, the analysis was limited to the reactant only, without considering individual products or estimating their kinetic parameters. This limitation prevents a comprehensive understanding of the system's behaviour, hindering both the detailed interpretation of the reaction network and the development of robust kinetic models needed for the design and optimization of reactors in complex heterogeneous catalytic processes.

The preliminary kinetic analysis using Eqs. (4)–(5) revealed that adsorption of all species in the transformation of  $\alpha$ -pinene epoxide had no significant influence on fitting the experimental data, as the determination coefficient ( $R^2$ ) only decreased slightly from 96.74% to 95.53%. This finding justified reducing the kinetic model from 12 to 8 parameters ( $k_1$ ,  $k_2$ ,  $k_3$ ,  $k_4$ ,  $E_{a1}$ ,  $E_{a2}$ ,  $E_{a3}$ ,  $E_{a4}$ ) by omitting the adsorption constants ( $K_{APO}$ ,  $K_{CA}$ ,  $K_{COL}$ ,  $K_{FA}$ ).

Initially, a kinetic model was considered in which all four surface reactions followed an unimolecular mechanism. In this case, the four rate expressions have the same form as Eq. (5) (see section 4.1.1 of the Supporting Information for details). Although this model yielded a relatively good coefficient of determination ( $R^2 = 94.32\%$ ), a comparison between the experimental data and the fitted model (kinetic parameters given in Table S6) revealed significant deviations at 40 °C (Fig. S9. a, e, and f). This behaviour suggests that a larger degree of curvature is needed to better capture the experimental trends. As a result, a bimolecular mechanism was proposed, leading to second-order dependence on concentration, as shown in Eq. (4). The best fit was achieved by considering bimolecular mechanisms for three of the four reactions, and a unimolecular mechanism for the remaining one.

Table 2 presents the optimized kinetic parameters for the isomerization of  $\alpha$ -pinene epoxide. The reaction rate constant ( $k_4$ ) estimated at 60 °C for the formation of byproducts (reaction 4) exhibited a very low value, which was an expected result due to the low selectivity of those compounds, generally below 5%, under the tested reaction conditions. On the other hand, the highest kinetic constant ( $k_1$ ) corresponded with the production of campholenic aldehyde, which is the major product in the  $\alpha$ -pinene epoxide isomerization over the dendritic ZSM-5 zeolite. The activation energies ranged from 75.1 to 80.4 kJ mol<sup>-1</sup>, observing that campholenic aldehyde has the lowest barrier energy in the reaction, while carveol has the highest one. Kinetic studies reported in the literature for the isomerization of  $\alpha$ -pinene oxide in *N,N*-dimethylacetamide at 140 °C over H-Beta-300 have obtained activation energy values for campholenic aldehyde, fencholenic aldehyde, and carveol of 81.8, 84.0, and 192 kJ mol<sup>-1</sup>, respectively. [35] In another kinetic study, which also evaluated activation energies for the main products, the reported values were 42 kJ mol<sup>-1</sup>, 48 kJ mol<sup>-1</sup>, 41 kJ mol<sup>-1</sup>, 66 kJ mol<sup>-1</sup>, and 43 kJ mol<sup>-1</sup> for campholenic aldehyde, fencholenic aldehyde, carveol, isopinocampheol, and pinocarveol, respectively. [33]

**Table 2**

Optimized kinetic parameters for the kinetic model for  $\alpha$ -pinene epoxide, considering a bimolecular mechanism.

Parameter	Value	Units	Standard error (%)
$k_1$	33.7	mL <sup>2</sup> mol <sup>-1</sup> mg <sup>-1</sup> min <sup>-1</sup>	3.6
$k_2$	13.2	mL <sup>2</sup> mol <sup>-1</sup> mg <sup>-1</sup> min <sup>-1</sup>	6.3
$k_3$	3.27	mL <sup>2</sup> mol <sup>-1</sup> mg <sup>-1</sup> min <sup>-1</sup>	21.1
$k_4$	$1.62 \times 10^{-4}$	mL mg <sup>-1</sup> min <sup>-1</sup>	12.8
$E_{a1}$	75.6	kJ mol <sup>-1</sup>	4.0
$E_{a2}$	80.4	kJ mol <sup>-1</sup>	5.7
$E_{a3}$	77.8	kJ mol <sup>-1</sup>	18.5
$E_{a4}$	75.1	kJ mol <sup>-1</sup>	31.4

$k_1$  values were estimated at 60 °C.

The comparison between experimental concentration profiles and those calculated using the kinetic model is illustrated in Fig. 6. These plots demonstrate that the proposed bimolecular kinetics effectively capture the experimental data, yielding a high  $R^2$  value of 95.53% and showing similar trends between the modeled and experimental curves. Additionally, all parameters exhibited small standard errors.

### 3.4.2. Kinetics of $\beta$ -pinene epoxide transformation

There are few kinetic studies available on the isomerization of  $\beta$ -pinene oxide, and most have focused on operating conditions or the formation of a single product. For instance, the work by Mäki-Arvela et al. (2013) presents an experimental analysis focused on conversion and product selectivity, reporting a global activation energy of 40 kJ mol<sup>-1</sup>, calculated from initial reaction rates over a temperature range of 27 to 70 °C, without developing a kinetic model or distinguishing individual formation pathways. [24] In contrast, Salminen et al. (2014) proposed a first-order pseudo-homogeneous kinetic model applied to catalysts with supported ionic liquids (SILCAs), which considers four parallel reaction pathways leading to myrtanal, myrtenol, perillyl alcohol, and other products. This allowed them to estimate individual activation energies for each pathway, although adsorption effects on the catalyst surface were not included. [33] Chaves-Restrepo et al. (2022), [32] in turn, employed two kinetic approaches, one based on a pseudo-homogeneous model and another of the Langmuir–Hinshelwood–Hougen–Watson (LHHW) type, to describe the reaction over iron-modified mesoporous catalysts. While adsorption effects were incorporated, the model was limited to a single reaction pathway leading to the formation of myrtanal, without considering secondary products or estimating activation energies. This restricts comprehensive analysis of the reaction network and makes it impossible to design and size a reactor based on simplified kinetic expressions that do not accurately represent the system phenomenology.

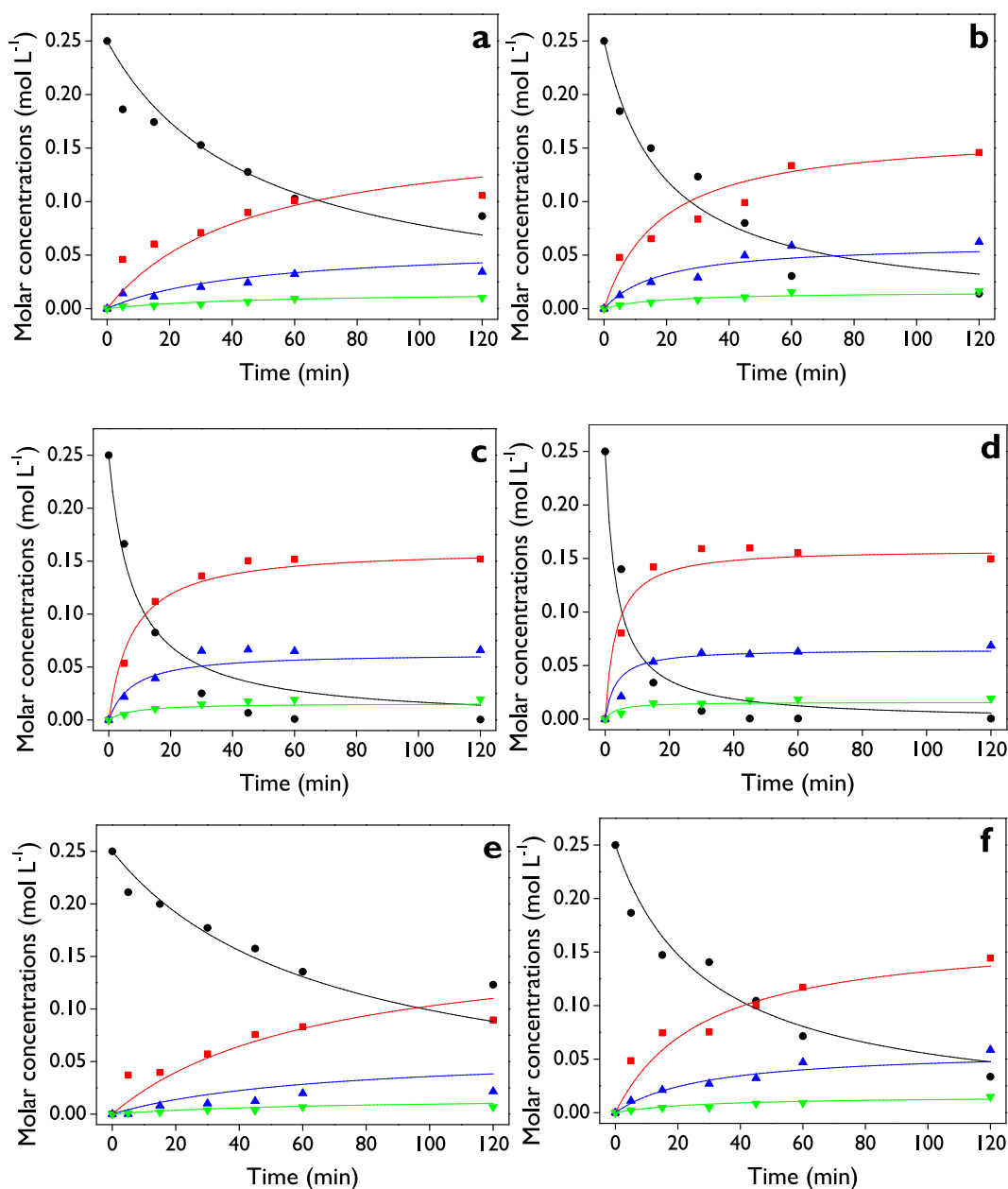
In the current study, a preliminary kinetic analysis using Eq. (6) revealed that the adsorption of the diastereoisomers of myrtanal represents the most influential adsorption constants in fitting the experimental data, where the same adsorption constant was assumed for both components ( $K_{CMAL} = K_{TMAL}$ ). Therefore, the final fitting involved the omission of the other adsorption constants in the denominator term of Eq. (6). Initially, like the isomerization of  $\alpha$ -pinene epoxide, a kinetic model considering all five surface reactions as unimolecular was evaluated. Although this model yielded a very high coefficient of determination ( $R^2 = 98.90\%$ ) and showed good agreement between the experimental data and the fitted model (Fig. S10; kinetic parameters are given in Table S7), it resulted in high standard errors of the kinetic constants (Table S7). Therefore, considering the strong fit obtained with the bimolecular mechanism for  $\alpha$ -pinene epoxide, this mechanism was also tested for the isomerization of  $\beta$ -pinene epoxide.

Table 3 presents the optimized kinetic parameters for the isomerization of  $\beta$ -pinene epoxide. The kinetic modelling revealed that the strong binding of cis- and trans-myrtanal to the catalyst significantly influences the final product distribution, as was observed previously in Figs. S2 and S4. This result is in line with previous reports in the literature. [9,36]

These kinetic parameters make it possible to rationalize the behaviours observed in the experiments by considering both adsorption aspects and formation rate. The selectivity towards the myrtanal isomers increased with rising temperature, while it decreased with increasing substrate concentration and catalyst loading. Although trans-myrtanal exhibits a slightly higher activation energy ( $E_{a2} = 64.4$  kJ mol<sup>-1</sup>) than cis-myrtanal ( $E_{a1} = 62.0$  kJ mol<sup>-1</sup>), its superior selectivity can be explained considering the kinetic rate constants, where trans-myrtanal has a higher formation rate constant ( $k_2 = 6.27$  mL<sup>2</sup> mol<sup>-1</sup> mg<sup>-1</sup> min<sup>-1</sup>) than the cis isomer ( $k_1 = 5.53$  mL<sup>2</sup> mol<sup>-1</sup> mg<sup>-1</sup> min<sup>-1</sup>), suggesting a faster reaction rate.

The reaction rate constant ( $k_3$ ) estimated at 60 °C for the formation of myrtenol exhibited the lowest value, as expected due to the low





**Fig. 6.** Concentration profiles of the species ( $C_{APO}$  (—, ●),  $C_{CA}$  (—, ■),  $C_{COL}$  (—, ▲),  $C_{FA}$  (—, ▼)) involved in the isomerization of  $\alpha$ -pinene epoxide over d-ZSM-5/7d catalyst, with experimental values (symbols) and modeled values (solid lines), considering a bimolecular mechanism. Reaction conditions: 0.25 mol L<sup>-1</sup> epoxide. (a) 40 °C and 10 mg of catalyst, (b) 50 °C and 10 mg of catalyst, (c) 60 °C and 10 mg of catalyst, (d) 70 °C and 10 mg of catalyst, (e) 40 °C and 7 mg of catalyst, (f) 40 °C and 16 mg of catalyst.

**Table 3**

Optimized kinetic parameters for the kinetic model for  $\beta$ -pinene epoxide, considering a bimolecular mechanism.

Parameter	Value	Units	Standard error (%)
$k_1$	5.53	ml <sup>2</sup> mol <sup>-1</sup> mg <sup>-1</sup> min <sup>-1</sup>	8.8
$k_2$	6.27	ml <sup>2</sup> mol <sup>-1</sup> mg <sup>-1</sup> min <sup>-1</sup>	8.6
$k_3$	1.05	ml <sup>2</sup> mol <sup>-1</sup> mg <sup>-1</sup> min <sup>-1</sup>	18.6
$k_4$	5.58	ml <sup>2</sup> mol <sup>-1</sup> mg <sup>-1</sup> min <sup>-1</sup>	8.7
$k_5$	5.64	ml <sup>2</sup> mol <sup>-1</sup> mg <sup>-1</sup> min <sup>-1</sup>	10.5
$Ea_1$	62.0	kJ mol <sup>-1</sup>	4.8
$Ea_2$	64.4	kJ mol <sup>-1</sup>	4.3
$Ea_3$	57.2	kJ mol <sup>-1</sup>	19.1
$Ea_4$	62.9	kJ mol <sup>-1</sup>	4.3
$Ea_5$	55.4	kJ mol <sup>-1</sup>	8.6
$K_{CMAL} = K_{TMAL}$	4.85	L mol <sup>-1</sup>	19.0

$k_i$  values were estimated at 60 °C.

selectivity observed for this compound over the dendritic zeolite, generally below 7%, under the tested reaction conditions. In contrast, the isomerization reactions leading to the formation of diastereoisomers of myrtanal showed high kinetic constants ( $k_1$  and  $k_2$ ), consistent with the fact that these are the major products. The activation energies ranged from 55.4 to 64.4 kJ mol<sup>-1</sup>, with similar values estimated for the myrtanal isomers (62.0 and 64.4 kJ mol<sup>-1</sup>). These results highlight the importance of understanding the specific reaction pathways in the isomerization of  $\beta$ -pinene epoxide, since kinetic studies on this transformation are still scarce. For example, a study with Beta and Y zeolites modified with Sn as catalysts reported only a global activation energy of 40 kJ mol<sup>-1</sup>, which corresponds to the total consumption of the epoxide, without detailing the kinetic profiles of each individual product. [24] In contrast, Salminen et al. (2014) carried out a more comprehensive kinetic modelling of the isomerization of  $\beta$ -pinene oxide using ionic liquids

supported on activated carbon fabric (SILCAs) as catalysts, to determine the specific activation energies for the products. They reported values of  $49 \text{ kJ mol}^{-1}$  for myrtanal,  $46 \text{ kJ mol}^{-1}$  for perillyl alcohol,  $48 \text{ kJ mol}^{-1}$  for myrtenol, and  $27 \text{ kJ mol}^{-1}$  for a mixture of unidentified products, called “others”. [33]

The comparison between the experimental concentration profiles and those determined by the kinetic model is shown in Fig. 7. These plots demonstrate that the proposed kinetics effectively capture the experimental behaviour, yielding a high  $R^2$  value of 98.22%, which is

comparable to that of the unimolecular kinetics (Table S7, Fig. S10). However, the standard errors for the bimolecular kinetics are now below 20%, significantly lower than those for the unimolecular kinetics (>50%, Table S7), suggesting greater reliability in the kinetic parameters obtained for the bimolecular model.

### 3.5. Catalyst robustness

The stability of the catalyst was assessed in the isomerization

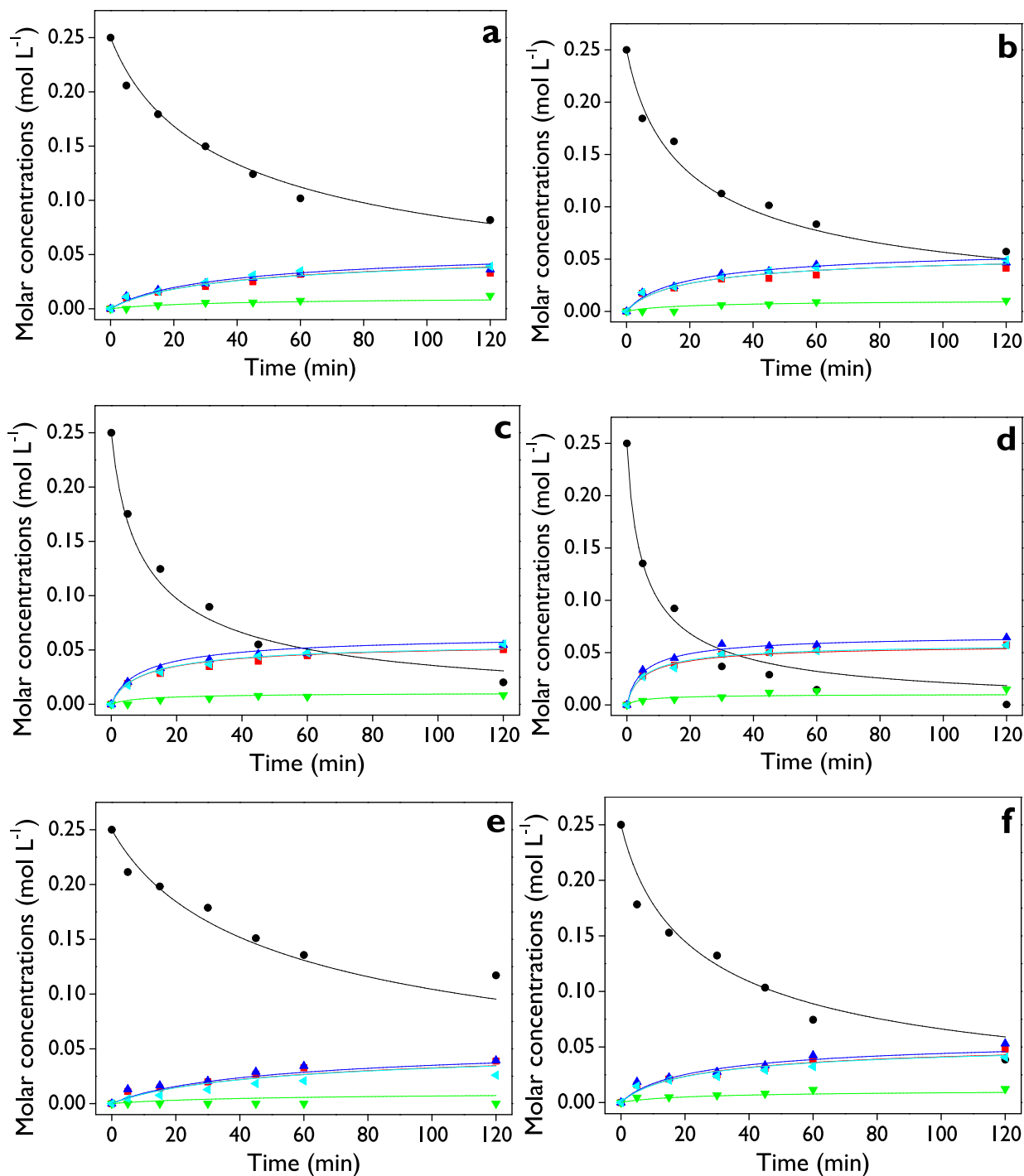


**Fig. 7.** Concentration profiles of the species ( $C_{BPO}$  (—, ●),  $C_{CMAL}$  (—, ■),  $C_{TMAL}$  (—, ▲),  $C_{MOL}$  (—, ▼),  $C_{PA}$  (—, ◀) involved in the isomerization of  $\beta$ -pinene epoxide over d-ZSM-5/7d catalyst, with experimental values (symbols) and modeled values (solid lines), considering a bimolecular mechanism. Reaction conditions:  $0.25 \text{ mol L}^{-1}$  epoxide. (a)  $40^\circ\text{C}$  and 10 mg of catalyst, (b)  $50^\circ\text{C}$  and 10 mg of catalyst, (c)  $60^\circ\text{C}$  and 10 mg of catalyst, (d)  $70^\circ\text{C}$  and 10 mg of catalyst, (e)  $40^\circ\text{C}$  and 7 mg of catalyst, (f)  $40^\circ\text{C}$  and 16 mg of catalyst.

reactions of  $\alpha$ - and  $\beta$ -pinene epoxides through leaching tests and catalyst reusability. The results obtained from the leaching tests (Fig. 8) indicated that the conversion of both epoxides remained constant after the catalyst was removed from the reaction medium, denoting that no leaching of the active species nor any contribution of homogeneous catalysis occurs during the process.

The reuse and regeneration tests of the dendritic zeolite in the isomerization of  $\alpha$ - and  $\beta$ -pinene epoxides are summarized in Table 4. After the reuse test, performed with the spent catalyst (washed with ethanol and dried), the conversion of  $\alpha$ - and  $\beta$ -pinene epoxides shows only slight variations, decreasing from 99.80 and 94.17% (fresh catalyst, Table 4) to 99.51 and 89.10% (Reuse 1, Table 4), respectively. These results indicate that, under the tested conditions, the catalyst essentially maintains its activity after reuse. Regarding selectivity, an increase is observed towards myrtanal, while campholenic aldehyde remains unchanged. This means that the myrtanal yield increases from 44.8% to 53.9%. In contrast, the selectivity towards alcohols such as perillyl alcohol and carveol decreases. This effect could be related to the presence of *cis*- and *trans*-myrtanal adsorbed on the catalyst surface, as suggested by the kinetic study, which may partially block the active sites responsible for perillyl alcohol formation. When the spent catalyst was regenerated by calcination (from room temperature to 400 °C at 1.8 °C min<sup>-1</sup> and held for 4 h, followed by heating to 550 °C at the same rate with a 5 h hold), both conversion and selectivity were fully recovered, showing values similar to those of the fresh catalyst. Therefore, the reuse test demonstrates that the dendritic zeolite remains highly active and selective after one cycle, while the regeneration by calcination in air allows the complete recovery of the slight changes observed in the catalytic performance.

### 3.6. Green metrics

Green chemistry metrics were used in this contribution as a quantitative tool to assess the environmental impact, efficiency, and sustainability of the isomerization of pinene epoxides. The metrics considered include atom economy (AE), reaction yield ( $\epsilon$ ), stoichiometric factor (SF), material recovery parameter (MRP), and reaction mass efficiency (RME). These metrics have been described by Andraos, [37–39] and the corresponding equations have been recently reported for the investigation of limonene-1,2-epoxide isomerization. [40] The metrics were evaluated under two scenarios: one considering the recovery of the catalyst and solvent, which is typical of laboratory-scale processes due to their ease of recovery via centrifugation, filtration, and/or rotary evaporation; the other considering the worst-case scenario where all

**Table 4**

Reuse and regeneration tests in the isomerization of  $\alpha$ - and  $\beta$ -pinene epoxide.

Run	APO			BPO		
	X (%)	S <sub>CA</sub> (%)	S <sub>COL</sub> (%)	X (%)	S <sub>MAL</sub> (%)	S <sub>PA</sub> (%)
Fresh	99.80	62.20	25.20	94.17	47.62	21.96
Reuse	99.51	62.35	19.63	89.10	60.44	12.67
Regeneration	99.70	63.22	25.01	96.22	50.44	24.15

Reaction conditions: 0.25 mol L<sup>-1</sup> of epoxide, ethyl acetate as the solvent, 10 mg of d-ZSM/7d, 70 °C, 1 h, 750 rpm. For the reuse test, the catalyst was separated by centrifugation at 4000 rpm for 5 min, washed with ethanol, and dried at 80 °C for 2 h. For the regeneration test, the spent catalyst was calcined after drying at 400 °C (1.8 °C min<sup>-1</sup>) for 4 h and 550 (1.8 °C min<sup>-1</sup>) for 5 h.

compounds are treated as waste. Fig. 9 presents the radial pentagon diagram for the three ZSM-5 catalysts investigated here in both epoxides isomerization, and Table S8 shows the values for each metric.

The atom economy is 100% for both  $\alpha$ - and  $\beta$ -pinene epoxide isomerization because the reaction is a rearrangement, meaning the molecular weight of the reactant and product remains the same. The stoichiometric factor is 1.0 since only the reactant undergoes transformation without any excess reagents. Notably, RME and MRP metrics are the most affected by the scenario: they are close to zero when catalyst and solvent are considered as waste, highlighting the low recovery and efficiency in such a case. However, these metrics increase significantly, approaching 1.0, when catalyst and solvent are recovered via centrifugation/filtration and rotary evaporation, owing to the substantial differences in boiling points between ethyl acetate and monoterpenoids.

The comparison between the three zeolites as catalysts was made after 30 min of reaction. Notably, the radial diagrams are very similar for both pinene epoxide systems using dendritic zeolites, demonstrating greener credentials compared to the hierarchical ZSM-5 sample. This is because the ideal green scenario is represented by a regular pentagon with each parameter equal to one, resulting in a unit-radius pentagon. The greener a reaction is, the closer the radial pentagon is to this ideal shape; conversely, the less green the reaction, the more the pentagon collapses towards the centre. RME and yield are higher for dendritic zeolites than for the hierarchical one, further highlighting their advantages. For instance, when comparing these two metrics for the three catalysts under the recovery scenario in the  $\alpha$ -pinene epoxide isomerization, the values are RME = 0.54, 0.59, 0.62, and  $\epsilon$  = 0.56, 0.61, 0.64 for h-ZSM-5, d-ZSM-5/4d, and d-ZSM-5-7d, respectively. Therefore, the green credentials of dendritic zeolites align with previous findings, [40]

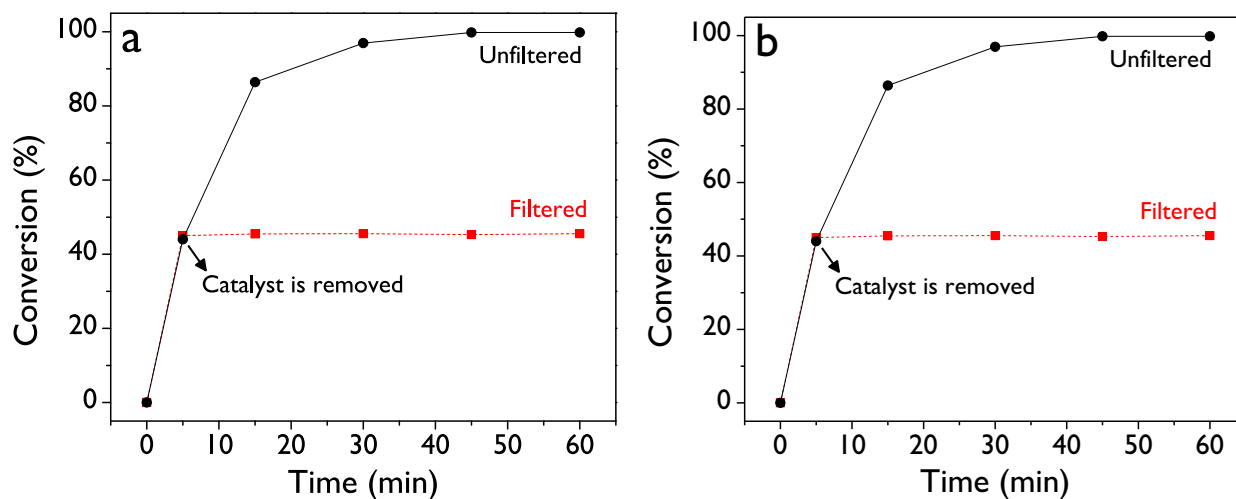


**Fig. 8.** Leaching test for (a)  $\alpha$ -pinene epoxide isomerization and (b)  $\beta$ -pinene epoxide isomerization over d-ZSM-5/7d catalyst. Reaction conditions:  $C_{\text{epoxide},0}$  = 0.25 mol L<sup>-1</sup>, 10 mg of catalyst, ethyl acetate as the solvent, 70 °C, 750 rpm.



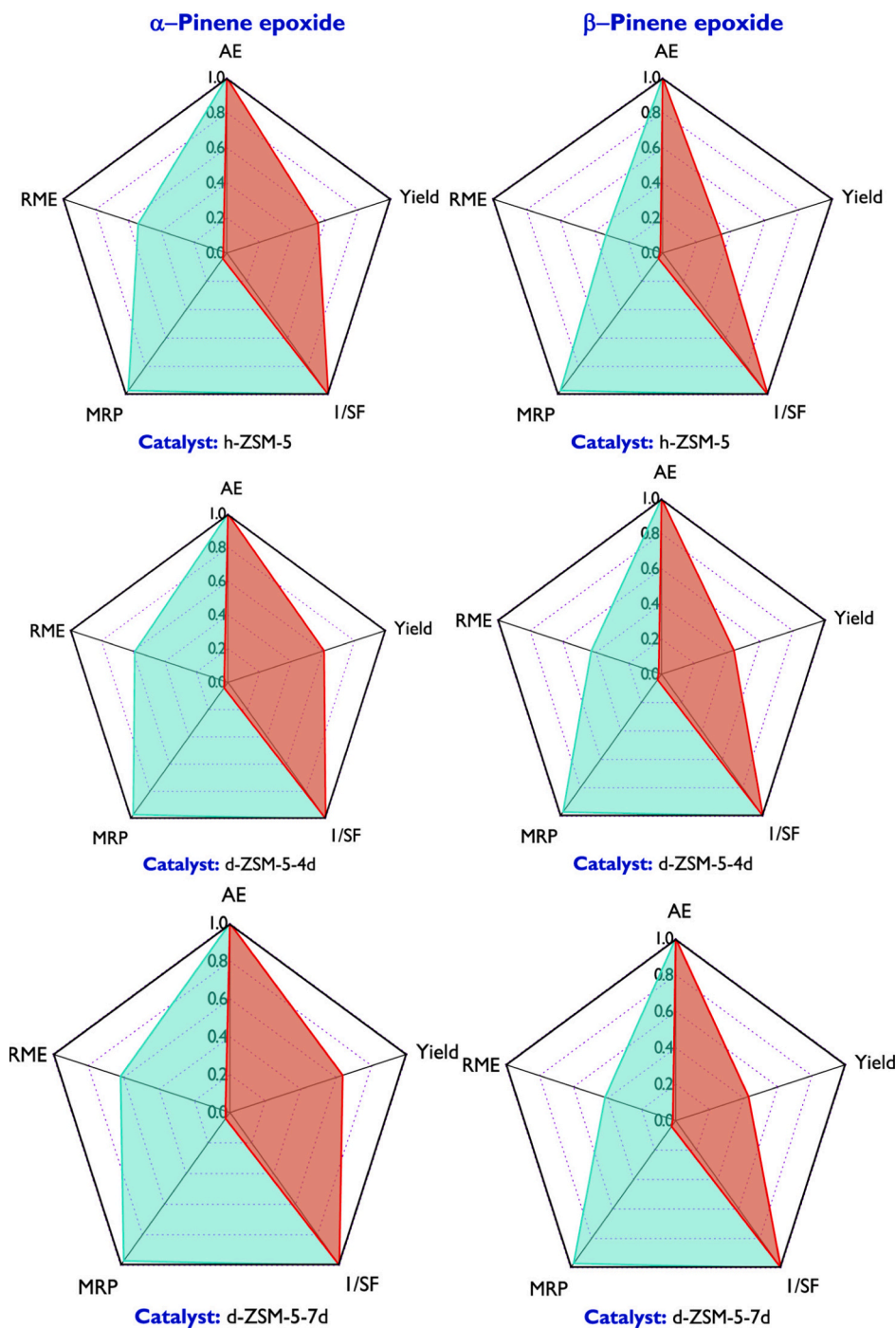


**Fig. 9.** Radial pentagon diagrams for the isomerization of  $\alpha$ - and  $\beta$ -pinene epoxides. Recovery scenario (—) and no recovery scenario (—). Reaction conditions: 0.25 mol L<sup>-1</sup> epoxide, ethyl acetate as the solvent, 10 mg catalyst, 70 °C, 30 min.

which also showed them to be very promising for the isomerization of limonene-1,2-epoxide into dihydrocarvone, a fine chemical important in several industries.

As observed, the green metrics obtained are promising for the valorisation of monoterpene epoxides, highlighting the importance of further research aimed at improving these metrics. In particular, the Reaction Mass Efficiency (RME) measures how much of the input materials are incorporated into the target product [40,41]. This shows that the process feasibility should be evaluated under conditions that minimize solvent usage, ideally considering a solvent-free system. Such optimization could lead to further improvements in the overall green metrics.

#### 4. Conclusions

This study highlights the potential of dendritic ZSM-5 zeolites as green catalysts for the isomerization of  $\alpha$ - and  $\beta$ -pinene epoxides under mild reaction conditions.  $\alpha$ -Pinene epoxide primarily yielded campholenic aldehyde and terpene alcohols, while  $\beta$ -pinene epoxide favoured monocyclic rearranged compounds. The results confirm that the dendritic nano-architecture of ZSM-5 sharply enhances accessibility to the active sites that, together with their balanced Brønsted-Lewis acidity, contribute to the high overall efficiency of the catalytic process. Thus, dendritic ZSM-5 samples exhibited in both reactions a superior performance than a hierarchical ZSM-5 material, used as a reference. Likewise,

the productivity so obtained over the dendritic zeolite catalysts demonstrated these materials as the most active catalysts reported in the literature to date in these reactions.

Catalyst robustness tests demonstrated that just slight variations in conversion and selectivity occur after the reuse of the dendritic ZSM-5 samples, being somewhat more marked in the case of  $\beta$ -pinene epoxides, while air calcination of the spent catalysts allowed the complete recovery of their activity and selectivity in the isomerization reactions of  $\alpha$ - and  $\beta$ -pinene epoxides. Additionally, no leaching of the active material was observed, ensuring the structural and chemical integrity of the catalyst during the usage cycles, making it suitable for application in heterogeneous processes with periodic regeneration.

The kinetic study confirmed the high rate of the chemical transformations leading to the predominant products formed from the  $\alpha$ - and  $\beta$ -pinene epoxide, which are campholenic aldehyde and myrtanal isomers, respectively, due to their lower activation energies. The slower kinetics observed in the conversion of  $\beta$ -pinene epoxide in comparison with the  $\alpha$ -isomer can be linked with the strong adsorption of *cis*- and *trans*-myrtanal on the catalyst, as confirmed by the kinetic analysis. This fact can also be related to the slight changes observed in the conversion/selectivity during the reusing test of  $\beta$ -pinene epoxide isomerization.

Better fitting with a bimolecular mechanism was observed for the isomerization of both epoxides, in agreement with the curvature observed in the experimental data and in contrast to the unimolecular mechanism previously reported for limonene-1,2-epoxide isomerization over a dendritic ZSM-5 zeolite. The preference for a bimolecular kinetic model may reflect a surface mechanism involving cooperative adsorption on both Lewis and Brønsted acid sites. Such dual-site interactions are known to enhance proton mobility and stabilize carbocation intermediates, thereby facilitating isomerization through a bimolecular pathway rather than a purely unimolecular rearrangement.

Evaluation of green metrics further confirmed the sustainable nature of the isomerization reaction using dendritic ZSM-5 zeolites, with more favourable values obtained in comparison with the hierarchical ZSM-5 sample.

#### CRediT authorship contribution statement

**Carina Mosquera:** Writing – original draft, Methodology, Investigation, Formal analysis. **Luis A. Gallego-Villada:** Writing – original draft, Software, Methodology, Investigation, Formal analysis, Conceptualization. **Marta Mediavilla:** Writing – original draft, Methodology, Investigation, Formal analysis. **Jennifer Cueto:** Writing – review & editing, Methodology, Investigation. **Maria del Mar Alonso-Doncel:** Methodology, Investigation. **Edwin Alarcón:** Supervision, Resources. **David P. Serrano:** Writing – review & editing, Validation, Supervision, Resources, Project administration, Funding acquisition.

#### Declaration of competing interest

The authors declare that they have no known competing financial interests or personal relationships that could have appeared to influence the work reported in this paper.

#### Acknowledgments

The authors are grateful to Universidad de Antioquia for funding project 2022-53000 as part of the “Convocatoria Programática 2021–2022: Ingeniería y Tecnología” program. Luis A. Gallego-Villada also acknowledges their financial support during his PhD studies through the “Beca Doctoral Universidad de Antioquia” scholarship. D.P. S., M.A.-D., and J.C. are gratefully acknowledged to the European Research Council Horizon 2020 research and innovation program TODENZE project (ERC101021502). It reflects only the author's view and the Agency ERCEA is not responsible for any use that may be made of the information it contains.

#### Appendix A. Supplementary data

The Supporting Information includes the experimental conditions for the kinetic modelling; investigation of different reaction conditions on the isomerization of both epoxides; calculations of internal mass transfer limitations; description of the kinetic modelling; data of catalyst characterization; benchmarking the productivity of dendritic zeolites; description of the reversibility tests; kinetic results; a summary of green metrics for the isomerization of  $\alpha$ - and  $\beta$ -pinene epoxides. Supplementary data to this article can be found online at <https://doi.org/10.1016/j.cej.2026.174355>.

#### Data availability

Data will be made available on request.

#### References

- [1] S. Cheng, X. Wang, Z. Deng, T. Liu, Innovative approaches in the discovery of terpenoid natural products, *Curr. Opin. Microbiol.* 83 (2025) 102575, <https://doi.org/10.1016/j.MIB.2024.102575>.
- [2] M. Kutyla, M. Pię, M. Stankevič, A. Junka, M. Brożyna, B. Dudek, R. Paduch, M. Trytek, Oxidation of myrtenol to myrtanal epoxide in a porphyrin-based photocatalytic system – A novel terpene alcohol derivative with antimicrobial and anticancer properties, *Bioorg. Chem.* 154 (2025) 108047, <https://doi.org/10.1016/j.BIOORG.2024.108047>.
- [3] G. Ranjani, S. Subramanian, X. Lopez-Lorenzo, M. Hakkarainen, P.-O. Syrén, Chemically recyclable and enzymatically degradable thermostable polyesters with inherent strain from  $\alpha$ -pinene-derived chiral diols, *ACS Sustain. Chem. Eng.* (2025), <https://doi.org/10.1021/acssuschemeng.5c01374>.
- [4] L.A. Gallego-Villada, E.A. Alarcón, F. Bustamante, A.L. Villa, One-Pot tandem catalysis: Green synthesis of  $\beta$ -pinene derivatives with MgO and mesoporous catalysts, *J. Catal.* 438 (2024) 115698, <https://doi.org/10.1016/j.jcat.2024.115698>.
- [5] T.B. Hughes, G.P. Miller, S.J. Swamidass, Modeling epoxidation of drug-like molecules with a deep machine learning network, *ACS Cent. Sci.* 1 (2015) 168–180, [https://doi.org/10.1021/ACSCENTSCI.5B00131/ASSET/IMAGES/LARGE/OC-2015-00131E\\_0011.JPEG](https://doi.org/10.1021/ACSCENTSCI.5B00131/ASSET/IMAGES/LARGE/OC-2015-00131E_0011.JPEG).
- [6] A. Corma, M. Renz, M. Susarte, Transformation of biomass products into fine chemicals catalyzed by solid lewis- and brønsted-acids, *Top. Catal.* 52 (2009) 1182–1189, <https://doi.org/10.1007/S11244-009-9266-5/SCHEMES/2>.
- [7] M. Stekrova, N. Kumar, A. Aho, I. Sinev, W. Grünert, J. Dahl, J. Roine, S. S. Arzumano, P. Mäki-Arvela, D.Y. Murzin, Isomerization of  $\alpha$ -pinene oxide using Fe-supported catalysts: Selective synthesis of campholenic aldehyde, *Appl. Catal. A Gen.* 470 (2014) 162–176, <https://doi.org/10.1016/J.APCATA.2013.10.044>.
- [8] E. Vrbková, E. Vyskočilová, M. Lhotka, L. Červený, Solvent influence on selectivity in  $\alpha$ -pinene oxide isomerization using MO3-modified Zeolite BETA, *Catalysts* 10 (2020) 1244, <https://doi.org/10.3390/CATAL10111244>. Page 1244 10 (2020).
- [9] H. Li, J. Liu, J. Zhao, H. He, D. Jiang, S.R. Kirk, Q. Xu, X. Liu, D. Yin, Selective Catalytic Isomerization of  $\beta$ -Pinene Oxide to Perillyl Alcohol Enhanced by Protic Tetraimidazolium Nitrate, *ChemistryOpen* 10 (2021) 477–485, <https://doi.org/10.1002/OPEN.202000318>.
- [10] A.S. Singh, D.R. Naikwadi, K. Ravi, A.V. Biradar, Chemoselective isomerization of  $\alpha$ -Pinene oxide to *trans*-Carveol by robust and mild Brønsted acidic zirconium phosphate catalyst, *Mol. Catal.* 521 (2022) 112189, <https://doi.org/10.1016/J.MCAT.2022.112189>.
- [11] M. Pitinova-Stekrova, P. Eliášová, T. Weissenberger, M. Shamzhy, Z. Musilová, J. Čejka, Highly selective synthesis of campholenic aldehyde over Ti-MWW catalysts by  $\alpha$ -pinene oxide isomerization, *Catal. Sci. Technol.* 8 (2018) 4690–4701, <https://doi.org/10.1039/C8CY01231H>.
- [12] M. Stekrova, N. Kumar, P. Mäki-Arvela, O.V. Ardashov, K.P. Volcho, N. F. Salakhutdinov, D.Y. Murzin, Selective preparation of *trans*-Carveol over ceria supported mesoporous materials MCM-41 and SBA-15, *Materials* 6 (2013) 2103–2118, <https://doi.org/10.3390/MA6052103>. Pages 2103–2118 6 (2013).
- [13] I. Paterova, B. Fidlerova, M. Vavra, E. Vyskočilova, L. Červený, Homogeneous Lewis and Brønsted acids as catalysts for  $\beta$ -pinene oxide rearrangement to prepare myrtenol and myrtanal, *Mol. Catal.* 492 (2020) 110945, <https://doi.org/10.1016/J.MCAT.2020.110945>.
- [14] A. Corma, M. Renz, M. Susarte, Transformation of Biomass Products into Fine Chemicals Catalyzed by Solid Lewis- and Brønsted-acids, *Top. Catal.* 52 (2009) 1182–1189, <https://doi.org/10.1007/s11244-009-9266-5>.
- [15] M.C. Cruz, J.E. Sánchez-Velandia, S. Causil, A.L. Villa, Selective synthesis of perillyl alcohol from  $\beta$ -pinene epoxide over Ti and Mo supported catalysts, *Catal. Lett.* 151 (2021) 2279–2290, <https://doi.org/10.1007/S10562-020-03489-1/FIGURES/10>.
- [16] V.V. Costa, K.A. Da Silva Rocha, L.F. De Sousa, P.A. Robles-Dutenhefner, E. V. Gusevskaya, Isomerization of  $\alpha$ -pinene oxide over cerium and tin catalysts: Selective synthesis of *trans*-carveol and *trans*-sobrerol, *J. Mol. Catal. A Chem.* 345 (2011) 69–74, <https://doi.org/10.1016/J.MOLCATA.2011.05.020>.

- [17] M. Puche Panadero, A. Velly, Readily available Ti-beta as an efficient catalyst for greener and sustainable production of campholenic aldehyde, *Cat. Sci. Technol.* 9 (2019) 4293–4303, <https://doi.org/10.1039/C9CY00957D>.
- [18] L.A. Gallego-Villada, J. Cueto, M. del M. Alonso-Doncel, P. Mäki-Arvela, E. A. Alarcón, D.P. Serrano, D.Yu. Murzin, Dendritic ZSM-5 zeolites as highly active catalysts for the valorization of monoterpene epoxides, *Green Chem.* 26 (2024) 10512–10528, <https://doi.org/10.1039/D4GC04003A>.
- [19] L.A. Gallego-Villada, W.Y. Perez-Sena, J.E. Sánchez-Velandia, J. Cueto, M. del Mar Alonso-Doncel, J. Wärnå, P. Mäki-Arvela, E.A. Alarcón, D.P. Serrano, D.Y. Murzin, Synthesis of dihydrocarvone over dendritic ZSM-5 Zeolite: A comprehensive study of experimental, kinetics, and computational insights, *Chem. Eng. J.* 498 (2024) 155377, <https://doi.org/10.1016/J.CEJ.2024.155377>.
- [20] M. del M. Alonso-Doncel, E.A. Giner, D. de la Calle, J. Cueto, P. Horcayada, R. A. García-Muñoz, D.P. Serrano, Synthesis of dendritic ZSM-5 zeolite through micellar templating controlled by the amphiphilic organosilane chain length, *Cryst. Growth Des.* 23 (2023) 5658–5670, [https://doi.org/10.1021/ACS.CGD.3C00326/ASSET/IMAGES/LARGE/CGC00326\\_0006.JPEG](https://doi.org/10.1021/ACS.CGD.3C00326/ASSET/IMAGES/LARGE/CGC00326_0006.JPEG).
- [21] M. del Mar Alonso-Doncel, C. Ochoa-Hernández, G. Gómez-Pozuelo, A. Oliveira, J. González-Aguilar, A. Peral, R. Sanz, D.P. Serrano, Dendritic nanoarchitecture imparts ZSM-5 zeolite with enhanced adsorption and catalytic performance in energy applications, *J. Energy Chem.* 80 (2023) 77–88, <https://doi.org/10.1016/J.JEchem.2023.01.023>.
- [22] N. Kumar, P. Mäki-Arvela, S.F. Díaz, A. Aho, Y. Demidova, J. Linden, A. Shepidchenko, M. Tenhu, J. Salonen, P. Laukkanen, A. Lashkul, J. Dahl, I. Sinev, A.R. Leino, K. Kordas, T. Salmi, D.Y. Murzin, Isomerization of  $\alpha$ -pinene oxide over iron-modified zeolites, *Top. Catal.* 56 (2013) 696–713, <https://doi.org/10.1007/S11244-013-0029-Y/FIGURES/19>.
- [23] J.E. Sánchez-Velandia, J.F. Gelves, L. Dorkis, M.A. Márquez, A.L. Villa, Ring-opening of  $\beta$ -pinene epoxide into high-added value products over Colombian natural zeolite, Microporous Mesoporous Mater. 287 (2019) 114–123, <https://doi.org/10.1016/J.MICROMESO.2019.05.053>.
- [24] P. Mäki-Arvela, N. Kumar, S.F. Díaz, A. Aho, M. Tenho, J. Salonen, A.R. Leino, K. Kordás, P. Laukkanen, J. Dahl, I. Sinev, T. Salmi, D.Y. Murzin, Isomerization of  $\beta$ -pinene oxide over Sn-modified zeolites, *J. Mol. Catal. A Chem.* 366 (2013) 228–237, <https://doi.org/10.1016/J.MOLCATA.2012.09.028>.
- [25] D. García, M. Jaramillo, F. Bustamante, A.L. Villa, E. Alarcón, Epoxidation of  $\beta$ -pinene with a highly-active and low-cost catalyst, *Braz. J. Chem. Eng.* 38 (2021) 89–100, <https://doi.org/10.1007/S43153-020-00078-Y/FIGURES/10>.
- [26] L.A. Gallego-Villada, E.A. Alarcón, A.L. Villa, Versatile heterogeneous catalytic system for the selective synthesis of limonene epoxide and diepoxide, *Ind. Eng. Chem. Res.* 62 (2023) 20152–20169, [https://doi.org/10.1021/ACS.IECR.3C02633/SUPPL\\_FILE/IE3C02633\\_SI\\_001.PDF](https://doi.org/10.1021/ACS.IECR.3C02633/SUPPL_FILE/IE3C02633_SI_001.PDF).
- [27] L.A. Gallego-Villada, E.A. Alarcón, C. Cerrutti, G. Blustein, Á.G. Sathicq, G. P. Romanelli, Levulinic acid esterification with n-butanol over a Preyssler catalyst in a microwave-assisted batch reactor: a kinetic study, *Ind. Eng. Chem. Res.* 62 (2023) 10915–10929, [https://doi.org/10.1021/ACS.IECR.3C00893/SUPPL\\_FILE/IE3C00893\\_SI\\_001.PDF](https://doi.org/10.1021/ACS.IECR.3C00893/SUPPL_FILE/IE3C00893_SI_001.PDF).
- [28] D.Y. Murzin, J. Wärnå, H. Haario, T. Salmi, Parameter estimation in kinetic models of complex heterogeneous catalytic reactions using Bayesian statistics, *React. Kinet. Mech. Catal.* 133 (2021) 1–15, <https://doi.org/10.1007/S11144-021-01974-1/TABLES/6>.
- [29] L.A. Gallego-Villada, E.A. Alarcón, Á.G. Sathicq, G.P. Romanelli, Kinetic modeling of microwave-assisted esterification for biofuel additive production: conversion of levulinic acid with pentanol using Dowex® 50WX8 catalyst, *React. Kinet. Mech. Catal.* 137 (2024) 2081–2103, <https://doi.org/10.1007/S11144-024-02657-3/TABLES/2>.
- [30] D.Y. Murzin, J. Wärnå, H. Haario, T. Salmi, Parameter estimation in kinetic models of complex heterogeneous catalytic reactions using Bayesian statistics, *React. Kinet. Mech. Catal.* 133 (2021) 1–15, <https://doi.org/10.1007/S11144-021-01974-1/TABLES/6>.
- [31] H. Haario, *ModEst User's guide*, 1994.
- [32] M. Chaves-Restrepo, A. Viloria, J.E. Sánchez-Velandia, A.L. Villa, Effect of reaction conditions and kinetics of the isomerization of  $\beta$ -pinene epoxide to myrtanal in the presence of Fe/MCM-41 and Fe/SBA-15, *React. Kinet. Mech. Catal.* 135 (2022) 2013–2029, <https://doi.org/10.1007/S11144-022-02220-Y/TABLES/4>.
- [33] E. Salminen, P. Mäki-Arvela, P. Virtanen, T. Salmi, J. Wärnå, J.P. Mikkola, Kinetics upon isomerization of  $\alpha$ , $\beta$ -pinene oxides over supported ionic liquid catalysts containing Lewis acids, *Ind. Eng. Chem. Res.* 53 (2014) 20107–20115, <https://doi.org/10.1021/IE503999Z;PAGE=STRING:ARTICLE/CHAPTER>.
- [34] J.E. Sánchez-Velandia, A. Agudelo-Cifuentes, A.L. Villa, Kinetics of the isomerization of  $\alpha$ -pinene epoxide over Fe supported MCM-41 and SBA-15 materials, *React. Kinet. Mech. Catal.* 128 (2019) 1005–1028, <https://doi.org/10.1007/S11144-019-01656-Z/FIGURES/10>.
- [35] P. Mäki-Arvela, N. Shcherban, C. Lozachmeur, V. Russo, J. Wärnå, D.Y. Murzin, Isomerization of  $\alpha$ -pinene oxide: solvent effects, kinetics and thermodynamics, *Catal. Lett.* 149 (2019) 203–214, <https://doi.org/10.1007/S10562-018-2617-8/FIGURES/7>.
- [36] E. Vyskočilová, J. Dušek, M. Babirádová, J. Krupka, I. Paterová, L. Červený, Perillyl alcohol preparation from  $\beta$ -pinene oxide using Fe-modified zeolite beta, *Res. Chem. Intermed.* 44 (2018) 3971–3984, <https://doi.org/10.1007/S11164-018-3335-Y/FIGURES/5>.
- [37] J. Andraos, Unification of reaction metrics for green chemistry: applications to reaction analysis, *Org. Process. Res. Dev.* 9 (2005) 149–163, [https://doi.org/10.1021/OP049803N/SUPPL\\_FILE/OP049803N.PDF](https://doi.org/10.1021/OP049803N/SUPPL_FILE/OP049803N.PDF).
- [38] J. Andraos, Application of Green Metrics Analysis to Chemical Reactions and Synthesis Plans, in: A. Lapkin, D. Constable (Eds.), *Green Chemistry Metrics: Measuring and Monitoring Sustainable Processes*, Blackwell Publishing Ltd, 2009.
- [39] J. Andraos, *Reaction Green Metrics: Problems, Exercises, and Solutions* - John Andraos - Google Libros, CRC Press., 2018.
- [40] L.A. Gallego-Villada, Green chemistry metrics: Insights from case studies in fine chemical processes, *Sustain. Chem. Pharm.* 46 (2025) 102062, <https://doi.org/10.1016/J.SCP.2025.102062>.
- [41] S.V. Quintana-Arturo, L.A. Gallego-Villada, E.A. Alarcón, D.Yu. Murzin, One-Pot Transformation of R-(+)-Limonene over Sr- and Sn-Modified Hierarchical Y Zeolite Catalysts: Toward Sustainable Conversion Routes, *ACS Sustain. Chem. Eng.* 13 (2025) 19790–19812, <https://doi.org/10.1021/acssuschemeng.5c08939>.